The Rotational Zeeman Effect of Methyl- and Silylbromide

K.-F. Dössel and D. H. Sutter

Abteilung Chemische Physik im Institut für Physikalische Chemie,
Universität Kiel, D-2300 Kiel

Z. Naturforsch. **34a**, 469–481 (1979); received Dezember 27, 1978

The rotational Zeeman effect of the $J \rightarrow J' = 0 \rightarrow 1$, $K = 0$ transition has been investigated for $CH_3{}^{81}Br$ and $SiH_3{}^{81}Br$ under high resolution. The shielding constant for the ^{81}Br-nucleus in these molecules has been determined from the spectra and is compared to the values calculated from the spin-rotation coupling constants. The sign of the electric dipole moment in SiH_3Br is shown to be $^{\oplus}H_3SiBr^{\ominus}$. From the Zeeman effect of two $K \neq 0$ transitions of SiH_3Br, $g_{\parallel}$ is determined to be negative for SiH_3Br, in contrast to CH_3Br, where $g_{\parallel}$ is positive.

Introduction

Although the rotational Zeeman effect has been observed for all symmetric top molecules of the type H_3C-X, where X is a halogen atom [1], the rotational spectra of the homologous silylcompounds H_3Si-X have not been observed in the presence of a magnetic field so far. Because the silicon atom can offer empty 3d-orbitals (in contrast to the carbon atom), a partial double bond character (pπ-dπ-bonding) is possible for the Si-X bond. This would lead to changes in the electron distribution of the molecule and hence to observable changes in the Zeeman parameters. So we decided to investigate the rotational Zeeman effect of silylbromide, $^{28}SiH_3{}^{81}Br$. To determine the direction of the electric dipolemoment we also investigated the rotational Zeeman effect of $^{28}SiD_3{}^{79}Br$.

Since Vanderhart and Flygare [1] in their work on the rotational Zeeman effect of CH_3Br measured only two Zeeman satellites which contain information on the Br-nuclear shielding σ_{av}, this value is determined very poorly there. Besides this, the Hamiltonian they used was incomplete and so we decided to reinvestigate the rotational Zeeman effect for CH_3Br.

The ^{81}Br-nuclear magnetic shielding has been predicted for CH_3Br and SiH_3Br from the spin-rotation coupling constants using the atomic dipole approximation [2]. The exact analysis of the observed Zeeman splittings for the first time offers the possibility to check the accuracy of this approximation for bromine compounds.

Reprint requests to Prof. Dr. D. H. Sutter, Institut für Physikalische Chemie der Universität Kiel Abt. Chemische Physik, Olshausenstraße 40–60, D-2300 Kiel. Es wird gebeten, womöglich Sonderdrucke zu bestellen statt die Arbeit zu kopieren.

0340-4811 / 79 / 0400-0469 $ 01.00/0

A. Silylbromide

Experimental

Silylbromide was prepared by reaction of hydrogenbromide with phenylsilane at −78 °C [3]. The spectra were recorded with a conventional 33 kHz square wave Stark effect modulated microwave spectrometer equipped with an electromagnet. Details of the design of the Zeeman microwave spectrometer may be found elsewhere [4]. The sample pressure was about 2 mTorr (0.2 Pascal) and the cell temperature about −70 °C. In the absence of the magnetic field all lines of $SiH_3{}^{81}Br$ and $SiH_3{}^{79}Br$ showed halfintensity halflinewidths (hhw's) of ~ 50 kHz, whereas some of the $SiD_3{}^{79}Br$ lines were considerably broadened with hhw's up to 150 kHz. This certainly is due to deuterium quadrupole coupling, which produces a further splitting of the hyperfine components [5]. Unfortunately this could not be resolved.

Theory

For the analysis of the rotational spectra of $SiH_3{}^{79}Br$ and $SiD_3{}^{79}Br$ in the absence of the magnetic field, we have used the same effective rotational Hamiltonian as in our previous work [3] on the rotational spectrum of $SiH_3{}^{81}Br$ with matrix elements in the coupled basis as given in Eq. (1) of Reference [3].

Because deuterium quadrupole coupling could not be resolved (see above), we neglected it in the analysis of the $SiD_3{}^{79}Br$ spectrum. The lower precision, which resulted from the deuterium line broadening, did not allow us to fit the ^{79}Br spin rotation coupling constants for $SiD_3{}^{79}Br$. In Tables 1 ($SiH_3{}^{79}Br$) and 2 ($SiD_3{}^{79}Br$) we give the observed zero field frequencies of the absorption lines, which we estimate to be accurate within

Table 1. Microwave spectrum of $SiH_3{}^{79}Br$. The observed frequencies (MHz) are compared to the values calculated from the molecular constants listed in Table 3 according to Equation (1) of Ref. [3].

J	K	$F \rightarrow F'$		ν_{obs}	obs-calc
0	0	3/2	5/2	8626.964	0.001
0	0	3/2	3/2	8710.803	−0.001
0	0	3/2	1/2	8560.118	−0.001
2	0	7/2	9/2	25926.638[a]	−0.001
2	0	5/2	7/2	25926.638[a]	0.019
2	0	3/2	5/2	25947.238	0.004
2	0	1/2	3/2	25947.404	−0.002
2	0	7/2	7/2	26010.406	−0.006
2	0	5/2	5/2	25887.739	−0.003
2	0	3/2	3/2	25863.394	0.005
2	1	7/2	9/2	25921.494	0.000
2	1	5/2	7/2	25942.325	−0.006
2	1	3/2	5/2	25942.938	−0.006
2	1	1/2	3/2	25921.896	0.004
2	1	7/2	7/2	25984.400	0.004
2	1	5/2	5/2	25913.087	−0.006
2	1	3/2	3/2	25880.186	0.001
2	2	7/2	9/2	25905.989	−0.010
2	2	5/2	7/2	25989.920	0.012
2	2	3/2	5/2	25930.104	−0.011
2	2	1/2	3/2	25846.447	0.006
2	2	7/2	7/2	25906.188	0.003
2	2	5/2	5/2	25989.714	−0.002
2	2	3/2	3/2	25930.433	0.004

[a] not resolved

Table 2. Microwave spectrum of $SiD_3{}^{79}Br$. The observed frequencies (MHz) are compared to the values calculated from the values calculated from the molecular constants listed in Table 3 according to Equation (1) of Ref. [3].

J	K	$F \rightarrow F'$		ν_{obs}	obs-calc
1	0	5/2	7/2	15303.563	−0.005
1	0	3/2	5/2	15303.500	−0.014
1	0	1/2	3/2	15394.503	−0.013
1	0	5/2	5/2	15387.162	−0.001
1	0	3/2	3/2	15244.213	0.002
1	0	1/2	1/2	15310.682	0.009
1	1	5/2	7/2	15290.398	−0.022
1	1	3/2	5/2	15374.252	0.015
1	1	1/2	3/2	15269.331	0.010
1	1	5/2	5/2	15332.434	0.008
1	1	3/2	3/2	15344.485	0.003
1	1	1/2	1/2	15227.740	−0.001
2	0	7/2	9/2	22961.987[a]	0.006
2	0	5/2	7/2	22961.987[a]	0.028
2	0	3/2	5/2	22982.512	0.004
2	0	1/2	3/2	22982.689	−0.014
2	1	7/2	9/2	22956.920	0.004
2	1	5/2	7/2	22977.692	0.009
2	1	3/2	5/2	22978.302	0.008
2	1	1/2	3/2	22957.287	0.004
2	2	7/2	9/2	22941.644	−0.012
2	2	5/2	7/2	23025.359	0.005
2	2	3/2	5/2	22965.692	−0.005
2	2	1/2	3/2	22882.248	0.015
3	0	9/2	11/2	30618.568[a]	−0.008
3	0	7/2	9/2	30618.568[a]	0.004
3	0	5/2	7/2	30628.214[a]	0.020
3	0	3/2	5/2	30628.214[a]	−0.034
3	1	9/2	11/2	30616.025	−0.002
3	1	7/2	9/2	30624.334	0.005
3	1	5/2	7/2	30628.676	0.002
3	1	3/2	5/2	30620.273	−0.005
3	2	9/2	11/2	30608.367	0.000
3	2	7/2	9/2	30641.693	0.001
3	2	5/2	7/2	30630.082	−0.003
3	2	3/2	5/2	30596.491	−0.001
3	3	9/2	11/2	30595.534	−0.016
3	3	7/2	9/2	30670.857	0.014
3	3	5/2	7/2	30632.327	−0.006
3	3	3/2	5/2	30557.273	0.007

[a] not resolved

Table 3. Molecular constants of silylbromide. The values for $SiH_3{}^{79}Br$ and $SiD_3{}^{79}Br$ result from a least squares fit to the spectra listed in Table 1 and 2. C_N and C_K could not be fitted for $SiD_3{}^{79}Br$ and were set equal to zero. The values for $SiH_3{}^{81}Br$ are taken from our previous work [3]. Uncertainties (in paranthesis) give one standard deviation and refer to the last figure quoted.

Isotopic species	$SiH_3{}^{81}Br$	$SiH_3{}^{79}Br$	$SiD_3{}^{79}Br$
B/MHz	4292.6462 (4)	4321.8019 (11)	3827.6791 (7)
D_{JK}/kHz	29.19 (4)	29.58 (14)	19.19 (8)
D_J/kHz	1.81 (1)	1.96 (6)	1.34 (3)
eqQ/MHz	279.825 (5)	334.981 (8)	334.158 (13)
C_N/kHz	−2.32 (40)	−0.6 (7)	—
C_K/kHz	−34.2 (11)	−28.0 (25)	—

better than ± 5 kHz for $SiH_3{}^{79}Br$ and ± 20 kHz for $SiD_3{}^{79}Br$. The uncertainty is entirely due to finite line widths. The result of the least squares fit of the molecular parameters to the observed frequencies is listed in Table 3. The last columns of Tables 1 and 2, which show the differences between the observed frequencies and those recalculated from the data of Table 3 according to Eq. (1) in [3], may be used as an indication of the quality of the fit.

In Tables 4 and 5 we give the observed Zeeman satellite frequencies for $SiH_3{}^{81}Br$ and $SiD_3{}^{79}Br$ resp., which were used to determine the molecular g-value $g_\perp$ and $g_\parallel$, the molecular susceptibility anisotropy $\chi_\perp - \chi_\parallel$, the shielded nuclear magnetic moment for the Br-nucleus, $g_I(1-\sigma_{av})I$, as well as the anisotropy of the ^{81}Br nuclear shielding, $(\sigma_\perp - \sigma_\parallel)$, (see Table 6) $(\sigma_{av} = (2\sigma_\perp + \sigma_\parallel)/3)$.

Table 4a. Zeeman splittings of the $J \to J' = 0 \to 1$, $K = 0$ rotational transition of $SiH_3{}^{81}Br$ (in MHz) at $H_0 = 21684$ G (see Fig. 2). The splittings are given relative to the hypothetical centre frequency of $\nu_c = 2B - 4D_J = 8585.285$ MHz.

$F \to F'$		$M_F \to$	M_F'	$\Delta\nu(H_0)$	$(H_{\text{eff}} - H_0)/G$	$\Delta\nu(H_{\text{eff}})$	$\Delta\nu_{\text{obs}}$	obs-cale
3/2	5/2	−1/2	1/2	−36.748	−18	−36.727	−36.697	0.030
		1/2	3/2	−25.924	−26	−25.907	−25.881	0.026
		−3/2	−5/2	−14.290	−38	−14.289	−14.309	−0.020
		3/2	5/2	−13.567	−38	−13.568	−13.574	−0.006
		−1/2	−3/2	− 6.151	−33	− 6.160	− 6.172	−0.012
		1/2	−1/2	3.214	−25	3.196	3.223	0.027
		3/2	1/2	13.093	−18	13.073	13.099	0.026
3/2	3/2	−3/2	−1/2	33.728	−23	33.746	33.754	0.008
		−1/2	1/2	40.134	−28	40.149	40.150	0.001
		1/2	3/2	43.591	−29	43.604	43.632	0.028
		−1/2	−3/2	72.936	−22	72.917	72.947	0.030
		1/2	−1/2	83.569	−15	83.546	83.538	−0.008
		3/2	1/2	89.975	−13	89.952	89.942	−0.010
3/2	1/2	−1/2	1/2	−105.714	−13	−105.691	−105.711	−0.020
		−3/2	−1/2	− 89.431	−19	− 89.410	− 89.393	0.017
		3/2	1/2	− 55.874	−28	− 55.889	− 55.896	−0.007
		1/2	−1/2	− 39.590	−17	− 39.611	− 39.606	0.005

Table 4b. Zeeman splittings of some rotational transitions of $SiH_3{}^{81}Br$ (in MHz). The splittings are given relative to the position of the unsplit line.

$J \to J' = 1 \to 2$, $F \to F' = 5/2 \to 7/2$, $K = 0$, $\nu_c = 17164.568$				
$H_{\text{av}} = 21.938$ kG	$M_F \to$	M_F'	$\Delta\nu_{\text{obs}}$	obs-calc
	−5/2	−7/2	−0.372	0.001
	5/2	7/2	0.338	−0.019
$H_{\text{av}} = 22.724$ kG	−5/2	−7/2	−0.396	−0.009
	5/2	7/2	0.368	−0.002
$H_{\text{av}} = 23.338$ kG	−5/2	−7/2	−0.402	−0.004
	5/2	7/2	0.366	−0.014
$J \to J' = 2 \to 3$, $F \to F' = 7/2 \to 9/2$, $K = 2$, $\nu_c = 25735.015$				
$H_{\text{av}} = 23.338$ kG	−7/2	−9/2	−1.404	−0.002
	7/2	9/2	1.326	−0.013
$J \to J' = 3 \to 4$, $F \to F' = 9/2 \to 11/2$, $K = 3$, $\nu_c = 34318.352$				
$H_{\text{av}} = 21.938$ kG	−9/2	−11/2	−1.898	−0.003
	9/2	11/2	1.837	−0.002
$H_{\text{av}} = 23.338$ kG	−9/2	−11/2	−2.017	0.001
	9/2	11/2	1.960	0.005

Table 5. Zeeman splittings of some rotational transitions of $SiD_3{}^{79}Br$ (in MHz). The splittings are given relative to the position of the unsplit line.

$J \to J' = 1 \to 2$, $F \to F' = 5/2 \to 7/2$, $K = 0$, $\nu_c = 15303.568$				
$H_{\text{av}} = 21.273$ kG	$M_F \to$	M_F'	$\Delta\nu_{\text{obs}}$	obs-calc
	−5/2	−7/2	−0.334	−0.001
	5/2	7/2	0.318	−0.001
$H_{\text{av}} = 22.866$ kG	−5/2	−7/2	−0.367	−0.006
	5/2	7/2	0.341	−0.002
$J \to J' = 2 \to 3$, $F \to F' = 7/2 \to 9/2$, $K = 0$, $\nu_c = 22961.981$				
$H_{\text{av}} = 21.273$ kG	−7/2	−9/2	−0.326	0.005
	7/2	9/2	0.317	−0.006
$H_{\text{av}} = 22.866$ kG	−7/2	−9/2	−0.377	−0.020
	7/2	9/2	0.338	−0.009
$J \to J' = 3 \to 4$, $F \to F' = 9/2 \to 11/2$, $K = 3$, $\nu_c = 30595.550$				
$H_{\text{av}} = 21.273$ kG	−9/2	−11/2	−0.720	0.010
	9/2	11/2	0.668	−0.008
$H_{\text{av}} = 22.866$ kG	−9/2	−11/2	−0.782	0.006
	9/2	11/2	0.750	0.026

For the analysis the effective rotational Hamiltonian given in Eq. (1) was used. In Eq. (1) $\mathcal{H}_{\text{rot}}$ is the standard symmetric

$$\mathcal{H}_{\text{eff}} = \mathcal{H}_{\text{rot}} + \mathcal{H}_{\text{Q}} + \mathcal{H}_{\text{SR}} + \mathcal{H}_{\text{g}}{}^{\text{mol}} + \mathcal{H}_{\text{g}}{}^{\text{nucl}} + \mathcal{H}_{\chi} + \mathcal{H}_{\text{TS}} \qquad (1)$$

top Hamiltonian including centrifugal distortion [6]. $\mathcal{H}_{\text{Q}}$ is the bromine nuclear quadrupole interaction Hamiltonian [7]. $\mathcal{H}_{\text{SR}}$ stands for the interaction of the Br-nuclear magnetic moment with the magnetic field produced by the overall rotation of the molecular charge distribution [3, 8, 9]. $\mathcal{H}_{\text{g}}{}^{\text{mol}}$ and $\mathcal{H}_{\chi}$ are the first and second order molecular Zeeman effect [8, 9]. $\mathcal{H}_{\text{g}}{}^{\text{nucl}}$ is the shielded nuclear Zeeman effect of the Br-nucleus [8, 9], and $\mathcal{H}_{\text{TS}}$ stands for the translational Stark effect [10], which originates from the Lorentz forces acting on the molecular charge distribution of molecules with non zero translational velocities with respect to the exterior field. Except for the bromine spin all other nuclear spins are neglected in $\mathcal{H}_{\text{eff}}$, since they are too loosely coupled to the overall rotation as to have a measurable effect on the rotational spectra (measurable within the present experimental

Table 6. Molecular Zeeman parameters as determined in a least squares fit to the experimental data of Table 4 (H_3SiBr), Table 5 (D_3SiBr), and Table 9 (H_3CBr). The $g_\parallel$-value of H_3CBr was taken from Ref. [1]. The paramagnetic contributions to the shielding, σ^p, have been calculated from the spin-rotation coupling constants [3], [15], and the diamagnetic contributions to the shielding, σ^d, were obtained by the atomic dipole approximation [2]. The nuclear magnetic moment of an unshielded bromine nucleus was taken to be $g_I\, I(^{81}Br) = 2.2692(5)$ [21] (see however Appendix II). $\sigma = \sigma^d + \sigma^p$.

	$H_3Si^{81}Br$	$D_3Si^{79}Br$	$H_3C^{81}Br$
$g_\perp$	−0.02185(13)	−0.02020(20)	−0.0057(3)
$g_\parallel$	−0.3185(5)	−0.1615(15)	+0.294(16)
$\frac{\chi_\perp - \chi_\parallel}{10^{-6}\,\mathrm{erg/G^2\,mol}}$	2.7(3)	2.5(9)	8.8(5)
$(1-\sigma_{av})g_I I$	2.2615(4)	—	2.2640(3)
σ_{av}/ppm	3569(616)	—	2467(572)
$(\sigma_\perp - \sigma_\parallel)$/ppm	$<\lvert 200\rvert$	—	−1110(956)
σ_{av}^{calc}/ppm	2817(39)	—	2502(11)
$(\sigma_\perp - \sigma_\parallel)^{calc}$/ppm	−85(63)	—	−784(20)
$\sigma_\perp^p$/ppm	−430(55)	—	−936(12)
$\sigma_\parallel^p$/ppm	−277(8)	—	−105(8)

resolution of the spectrometer). The Hamiltonian matrix corresponding to Eq. (1) was set up in the uncoupled basis $|J, K, I, M_J, M_I\rangle$ where J, K, and M_J are the usual symmetric top quantum number and where I and M_I refer to the bromine spin and its projection in direction of the exterior magnetic field which is used as quantization axis. The non-vanishing matrix elements of $\mathscr{H}_{eff}$ that were used in this work are listed in the Appendix I. The matrix elements of $\mathscr{H}_{SR}$ and $\mathscr{H}_g{}^{mol}$ off diagonal in M_J and M_I, which we did not find in the literature, were calculated by use of the Wigner-Eckart theorem.

If the Hamiltonian matrix is set up in the uncoupled basis it factorizes, at least to a first approximation, into submatrices which correspond to different rotational states characterized by the rigid rotor quantum numbers J and K. Depending on J, these submatrices are of rank $(2J+1)(2I+1)$ corresponding to the different M_J and M_I values. From the matrix elements which connect the different J, K-submatrices only those due to $\mathscr{H}_Q$ are sufficiently large to have a measurable, though small effect on the rotational levels. This allowed us to treat every J, K-block separately after the relevant off diagonal elements of $\mathscr{H}_Q$ had been projected into it by a Van Vleck Transformation [11].

With the applied fields between 9 and 22 kG, the matrix elements of $\mathscr{H}_g{}^{mol}$ and $\mathscr{H}_g{}^{nucl}$, which are diagonal in M_J and M_I, are comparable in magnitude to the matrix elements of $\mathscr{H}_Q$, which are both diagonal and off diagonal in M_J and M_I. Thus mixing of different M_J, M_I-states is rather strong, and M_J and M_I loose their meaning as projection quantum numbers for the rotational and spin angular momenta. Indeed Fig. 1 shows, that for

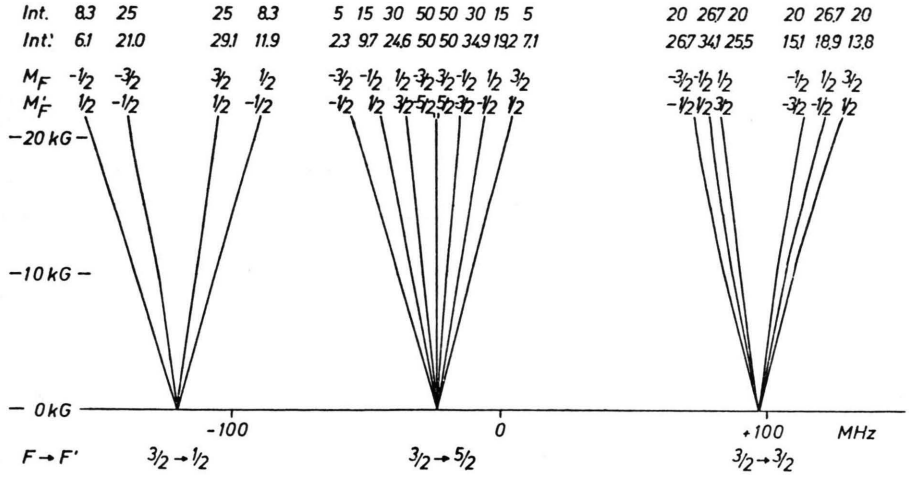

Fig. 1. Calculated field dependence of the Zeeman pattern of the $J \rightarrow J' = 0 \rightarrow 1$, $K = 0$ transition of $CH_3{}^{81}Br$ (compare Table 9). The calculation is based on the Hamiltonian given in Eq. (1) (see text) and the molecular parameters given in Tables 6 and 8. In view of the fairly symmetric splittings the quantum numbers of the limiting coupled basis are still used to characterize the different satellites. Rather strong deviations of the satellite intensities calculated for 21.7 kG, Int'., from their values in the limit of very low fields, Int., however indicate the change to the intermediate coupling case. (Intensities are given in arbitrary units).

$CH_3{}^{81}Br$ (and the same holds for $SiH_3{}^{81}Br$) the quantum numbers of the coupled basis, F and M_F can still be used to characterize the observed transitions. A further, but much smaller mixing of M_J, M_I-states is induced by those matrix elements of $\mathscr{H}_Q$, which are off diagonal in J and were folded into the J, K-block under consideration in a second order perturbation treatment. Finally for $K+0$ levels the translational Stark effect $\mathscr{H}_{TS}$ produces a mixing between states differing in M_J by ± 1. For every J, K-block the Hamiltonian matrix was diagonalized numerically.

With the magnetic field perpendicular to the electric field vector of our microwave radiation, there are for every rotational transition two of the Zeeman components, whose shift from their zero field position is independent of $\mathscr{H}_Q$ and $\mathscr{H}_g{}^{nucl}$. The special properties of these transitions with $F = I + J \rightarrow F' = I + J + 1$; $M_F = \pm F \rightarrow M_F' = \pm F'$ (or in the uncoupled basis $J \rightarrow J + 1$; $M_J = \pm J$, $M_I = \pm I \rightarrow M_J' = \pm J \pm 1$, $M_I = \pm I$) have been described elsewhere [1, 12]. We note, that these transitions allow one to determine $g_\perp$, $g_\parallel$ $(\chi_\perp - \chi_\parallel)$, and $(\sigma_\perp - \sigma_\parallel)$, but contain no information on the signs of $g_\perp$ and $g_\parallel$ or the value of the average chemical shielding σ_{av} at the Br-nucleus.

We analyzed the Zeeman effect of all hyperfine components of the $J \rightarrow J' = 0 \rightarrow 1$, $K = 0$ rotational transition of $SiH_3{}^{81}Br$ to determine the value of $\sigma_{av} = \frac{1}{3}(\sigma_\parallel + 2\sigma_\perp)$ and the sign of $g_\perp$ relative to the known sign of the bromine nuclear g-value [13]. For $SiH_3{}^{81}Br$ the relative sign of $g_\perp$ and $g_\parallel$ was determined unambiguously from the rotational Zeeman effect of the $J \rightarrow J' = 2 \rightarrow 3$, $K = 2$, $F \rightarrow F' = 7/2 \rightarrow 9/2$, $M_F \rightarrow M_{F'} = \pm 7/2 \rightarrow \pm 9/2$ and $J \rightarrow J' = 3 \rightarrow 4$, $K = 3$, $F \rightarrow F' = 9/2 \rightarrow 11/2$, $M_F \rightarrow M_{F'} = \pm 9/2 \rightarrow \pm 11/2$ transitions. For the $SiD_3{}^{79}Br$ isotope the signs of $g_\parallel$ and $g_\perp$ must be the same as for the $SiH_3{}^{81}Br$ isotope (compare Eq. (3) below).

Effect of Field Inhomogeneity

As is shown in Fig. 2 the magnetic field is not constant over the absorption path but decreases towards the ends of the magnet. This field inhomogeneity leads to a deformation and shift of the recorded absorption lines, which depends on

a) the magnetic field profile,

b) the sensitivity of the absorption frequency to the applied field $d\nu_i/dH$ and

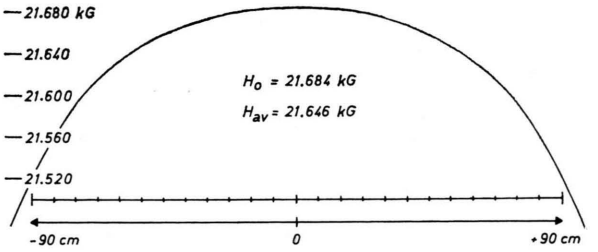

Fig. 2. The longitudinal drop of the magnetic field towards the ends of the magnet limits the usable gap volume. Only the central 180 cm (= length of the septum used to Stark-modulate the molecular absorption) were used in the present study. The field was measured with a Rawson & Lush rotating coil Gaussmeter type 920 M.

c) the linewidth (mainly due to molecule/molecule and molecule/wall collision broadening).

If the inhomogeneity of ~ 150 Gauss shifts the frequency of the satellite under consideration by less than approximately one half of the half intensity linewidth (typically 50 kHz), then the experimental line shape still looks fairly symmetric and the evaluation of the Zeeman satellite frequency may be based on the average value of the magnetic field averaged over the full absorption length.

If on the other hand the Zeeman satellite frequency shows a very strong field dependence, the profile of the absorption line becomes asymmetric with a steep slope at the "high field side" and tailing off to the "low field side" as is illustrated in Figure 3. In such cases the peak of the recorded

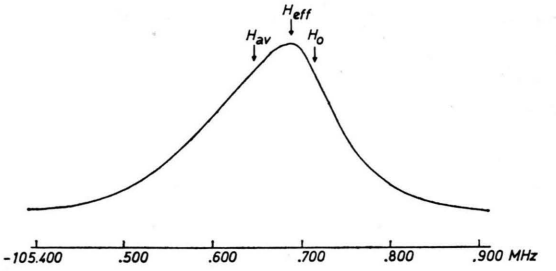

Fig. 3. Calculated line profile of the $J \rightarrow J' = 0 \rightarrow 1$, $K = 0$, $F \rightarrow F' = 3/2 \rightarrow 1/2$, $M_F \rightarrow M_{F'} = -1/2 \rightarrow 1/2$ transition of $H_3Si^{81}Br$. Due to the inhomogeneity of the magnetic field (see Fig. 2) and the high sensitivity of this satellite on the magnetic field ($d\nu/dH = -1.79$ kHz/G) the line shape becomes asymmetric. For the maximum field of $H_0 = 21.684$ kG the shift of the absorption frequency with respect to the hypothetical centre frequency is $\Delta\nu = -105.713$ MHz. For the averagefield, $H_{av} = 21.646$ kG, it lies 68 kHz above this frequency. The maximum of the absorption intensity shown here corresponds to an effective magnetic field, H_{eff}, which is given in Tables 4 and 9 for every satellite.

absorption neither corresponds to the maximum field strength H_0, reached in the centre of the gap, nor to the average magnetic field H_{av}, but to an intermediate "effective field", which was determined as follows.

In a first fit the observed Zeeman satellite frequencies were used together with the experimentally determined average field values to get initial values for the susceptibility anisotropy, the $g_\perp$ and $g_\parallel$ values etc. Before the second fit the observed field profile was approximated by a step profile by subdividing the absorption volume into 24 segments of equal length and by approximating the field within each of the segments by its value in its centre. Then the Zeeman parameters determined in the first fit were used to calculate theoretical line profiles as superpositions of Zeeman satellites originating from the different segments according to Equation (2).

$$I_i(\nu) = \sum_{l=1}^{24} \frac{b}{(\nu - \nu_i(H_l))^2 + b^2}, \qquad (2)$$

$I_i(\nu)$ = absorption intensity of i-th Zeeman satellite ν_i at frequency ν (arbitrary scale),

b = half intensity half width determined experimentally from the zero field line profiles (50 kHz),

$\nu_i(H_l)$ = satellite frequency for the segment field strength H_l of the l-th segment.

As an example the result of such a calculation is shown in Fig. 3 for the $J \to J' = 0 \to 1$, $K = 0$, $F \to F' = 3/2 \to 1/2$, $M_F \to M_F' = -1/2 \to 1/2$ rotational transition of $SiH_3{}^{81}Br$, for which $d\nu_i/dH = -1.79$ kHz/G. As is seen from the Fig. 3, the peak frequency of the absorption profile is shifted from the value calculated for a homogeneous field H_0 (centre gap value) to a frequency that was calculated for a slightly lower effective value of the magnetic field, H_{eff}. These effective field values were used in the final least squares fit of the Zeeman parameters to the observed peak frequencies of the Zeeman satellites.

As can be shown, the procedure described above accounts for the fact, that in the least squares fit of the Zeeman parameters [14] each observed Zeeman satellite frequency does not correspond to a single normal equation, but to a whole set, whose members originate from the different segments of the absorption cell. In cases where the spread of the satellite frequency corresponding to the fields in the different segments is small with respect to the linewidth, b, these equations are lumped together with essentially equal weight, while in cases of satellites with stronger field dependence, they are lumped together with different weights, decreasing with increasing deviation from the centre gap frequency.

B. Methylbromide

We recorded the $J \to J' = 0 \to 1$, $K = 0$ (compare Fig. 1) and $J \to J' = 1 \to 2$, $K = 0$ rotational transitions of $CH_3{}^{81}Br$ under field free conditions (see Table 7). As for SiH_3Br, we used Eq. (1) of [3] to determine B_0, D_J, eqQ, and $C_\perp$ from the observed frequencies (see Table 8). The molecular constants obtained here agree with those given by

Table 7. Microwave spectrum of $CH_3{}^{81}Br$. The observed frequencies (MHz) are compared to the values calculated from the molecular constants listed in Table 8 according to Equation (1) of Ref. [3].

J	K	$F \to F'$		ν_{obs}	obs-calc
0	0	3/2	5/2	19039.647	0.001
0	0	3/2	3/2	19160.243	0.001
0	0	3/2	1/2	18943.312	−0.004
1	0	5/2	7/2	38116.729	−0.009
1	0	3/2	5/2	38116.684	0.003
1	0	1/2	3/2	38247.792	0.004
1	0	5/2	5/2	38237.280	0.002
1	0	3/2	3/2	38030.862	0.000
1	0	1/2	1/2	38126.982	0.000
1	0	5/2	3/2	38151.452	−0.006
1	0	3/2	1/2	37910.060	0.005

Table 8. Molecular constants of methylbromide. The values in the first column result from a least squares fit to the spectrum listed in Table 6. Since no $K \neq 0$ lines were measured here, D_{JK} and C_K could not be determined. The values in the second column are from the work of Demaison et al. [15], who measured high J transitions. The results agree within two standard deviations but eQq is determined more accurately here.

	this work	Ref. [15]
B/MHz	9531.834(2)	9531.8304(7)
D_J/kHz	10.3(3)	9.7960(14)
D_{JK}/kHz	—	127.836(6)
eQq/MHz	482.141(8)	482.13(14)
C_N/kHz	−12.0(9)	−13.78(19)
C_K/kHz	—	−25.4(20)

Table 9. Zeeman splittings of the $J \rightarrow J' = 0 \rightarrow 1$, $K = 0$ rotational transition of $CH_3{}^{81}Br$ (in MHz). The splittings are given relative to the hypothetical centre frequency of $\nu_c = 2B - 4D_J = 19063.627$ MHz. $H_0 = 21691$ G.

$F \rightarrow$	F'	$M_F \rightarrow$	M_F'	$\Delta\nu(H_0)$	$(H_{\text{eff}} - H_0)/G$	$\Delta\nu(H_{\text{eff}})$	$\Delta\nu_{\text{obs}}$	obs − calc
3/2	5/2	−3/2	−1/2	−55.648	−15	−55.625	−55.619	0.006
		−1/2	1/2	−45.669	−19	−45.649	−45.652	−0.003
		1/2	3/2	−35.149	−27	−35.133	−35.121	0.012
		−3/2	−5/2	−24.136	−38	−24.135	−24.125	0.010
		3/2	5/2	−23.959	−38	−23.960	−23.962	−0.002
		−1/2	−3/2	−15.250	−31	−15.261	−15.275	−0.014
		1/2	−1/2	− 5.752	−23	− 5.770	− 5.756	0.014
		3/2	1/2	4.226	−17	4.205	4.206	0.001
3/2	3/2	−3/2	−1/2	71.742	−20	71.762	71.753	−0.009
		−1/2	1/2	78.292	−25	78.318	78.309	−0.009
		1/2	3/2	83.008	−27	83.024	83.033	0.009
		−1/2	−3/2	112.799	−23	112.781	112.782	0.001
		1/2	−1/2	121.638	−16	121.617	121.611	−0.006
		3/2	1/2	128.188	−14	128.166	121.179	0.013
3/2	1/2	−1/2	1/2	−155.147	−13	−155.125	−155.113	0.012
		−3/2	−1/2	−138.619	−21	−138.599	−138.585	0.014
		3/2	1/2	−105.251	−27	−105.268	−105.271	−0.003
		1/2	−1/2	− 88.723	−16	− 88.745	− 88.736	0.009

Demaison et al. [15] to within two standard deviations, but only eqQ is determined more accurately here.

In Table 9 we give the observed Zeeman satellite frequencies for $CH_3{}^{81}Br$, which we used to determine the molecular g-value $g_\perp$, the molecular susceptibility anisotropy $(\chi_\perp - \chi_\parallel)$ the shielded nuclear magnetic moment for the Br-nucleus $(1 - \sigma_{\text{av}})g_I I$, and the anisotropy in the nuclear magnetic shielding $(\sigma_\perp - \sigma_\parallel)$. In the analysis of the experimental data we used the Hamiltonian of Equation (1).

C. Discussion

Isotopic Variation of eqQ

The ratio of the quadrupole coupling constants, eqQ, for the two isotopic species $SiH_3{}^{79}Br/SiH_3{}^{81}Br$ and $CH_3{}^{79}Br/CH_3{}^{81}Br$ is found to be

$$eqQ_{(SiH_3{}^{79}Br)}/eqQ_{(SiH_3{}^{81}Br)} = 1.19711(4) \quad \text{and}$$
$$eqQ_{(CH_3{}^{79}Br)}/eqQ_{(CH_3{}^{81}Br)} = 1.19703(4).$$

These values are in good agreement with the tabulated value for the ratio of the nuclear quadrupole moments $Q_{(^{79}Br)}/Q_{(^{81}Br)} = 1.19707(3)$ [16]. The differences in the ratios are not significant. There is however a small 0.25% difference in the effective bromine nuclear quadrupole coupling constants in $SiH_3{}^{79}Br$ and $SiD_3{}^{79}Br$. We believe that this difference is due to different zero point vibrational averaging in the two isotopes. To check this hypothesis, it would be necessary to combine a normal coordinate analysis with experimental eqQ-values of molecules in excited states of the different vibrational modes, an investigation which was beyond the scope of the present study.

Sign of the Molecular Electric Dipole Moment in SiH_3Br

The rotational g-factors, when measured for two isotopic species of a molecule, can be used to give the sign of, and the approximate magnitude of the electric dipole moment. For an isotopic substitution, which shifts the centre of gravity along the symmetry axis z by Δz, so as to change all z-coordinates from z_n to $z_n' = z_n + \Delta z$ and to change the moments of inertia, $I_\perp = \hbar/8\pi^2 B$, and the $g_\perp$-values to $I_\perp'$ and $g_\perp'$ resp., we have [17]:

$$\frac{e}{2M_p}(g_\perp' I_\perp' - g_\perp I_\perp) \tag{3}$$
$$= \frac{e\hbar}{16\pi^2 M_p}(g'/B' - g/B) = \Delta z\, \mu_z$$

where e is the proton charge and M_p the proton mass. If we take $D_3Si^{79}Br$ as the primed species and $SiH_3{}^{81}Br$ as the unprimed species together with the structural data $r_{SiH} = 1.485$ Å, $r_{SiBr} = 2.210$ Å, and $\sphericalangle HSiBr = 107.8°$ [31], the shift of the centre of mass is calculated as $\Delta z = 0.065_5$ Å. (The

positive z-Axis is assumed to point towards the bromine atom.) Insertion of the rotational constants (Table 3) and $g_\perp$-values (Table 6) then leads to a value of $\mu_z = -3.4 \pm 1.6$ D, i.e. $^+H_3SiBr^-$. This value has to be compared to the absolute value of the dipole moment, $|\mu_z| = 1.318 \pm 0.008$ D [3], determined with considerably higher accuracy from the Stark-effect. Although the Zeeman value is 1.3 standard deviations off the Stark-effect value, we are confident that it gives the correct sign of the dipole moment.

Sign of $g_\parallel$ in Silylcompounds

It has been demonstrated by Vanderhart and Flygare [1], that the sign and magnitude of the rotational g-factor associated with the rotation of a methyl group about its symmetry axis ($g_\parallel$ for all methyl halides) is approximately $g_{\parallel(CH_3^-)} = +0.31$. For SiH_3Br the present study has shown, that the corresponding g-factor associated with the rotation of a silyl group has about the same absolute value but the opposite sign: $g_{\parallel(SiH_3^-)} = -0.32$. Further examples are silane, where a g-factor of $g_{(SiH_4)} = -0.27$ was observed [18], and H_3C-SiH_3, where the contributions from the methyl- and silylgroups nearly cancel to give a very small $g_\parallel$ of $g_{\parallel(H_3CSiH_3)} = \pm 0.018$ [19]. In a simple model of point charges (see Fig. 4) the observation of a positive $g_\parallel$-factor for the methyl group and of a negative $g_\parallel$-factor for the silyl group can be "explained" by assuming opposite charges on the off-axis H-atoms. These opposite polarities in the C—H and Si—H bonds have been predicted from the different electronegativities of the atoms (2.5 for carbon, 2.15 for hydrogen, and 1.8 for silicon resp. [20].

^{81}Br Nuclear Shielding

From the experimentally determined $(1-\sigma_{av})g_I I$ values of $SiH_3{}^{81}Br$ and $CH_3{}^{81}Br$ we can calculate the ^{81}Br nuclear shielding in both molecules (see Table 6). In this calculation the unshielded nuclear magnetic moment of the bare ^{81}Br nucleus was taken to be $g_I I = 2.2696(5)$ [21] (however see Appendix II). The errors given for $(1-\sigma_{av})g_I I$ and $g_I I$ are one standard deviation and reflect the (statistical) uncertainties in the frequency measurements leading to these values. Besides this there is an additional uncertainty in the measurement of the magnetic field, which is approximately ± 5 Gauss at 20 kG. This leads to a systematic error in the

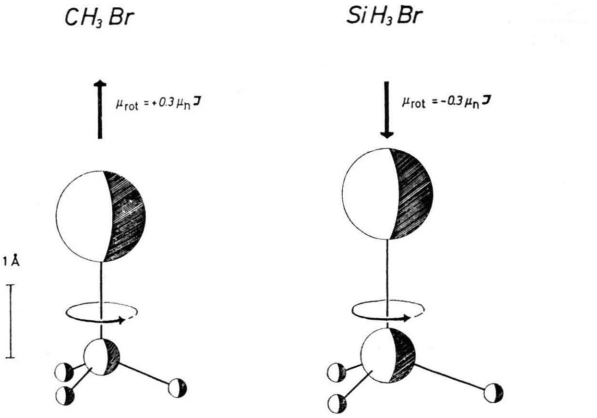

Fig. 4. Like the electric current in a closed loop of wire, the rotation of charges in a molecule will leed to an observable magnetic moment. The orientation of the magnetic moment produced by a rotation of the methylgroup as e.g. in CH_3Br is found to be parallel to the angular momentum vector. In the simple model of point charges, this means that the hydrogen atoms, which lie off the axis of symmetry, are carrying a partial positive charge. For the silylgroup as e.g. in SiH_3Br the magnetic moment and the angular momentum vector are found to be antiparallel. This then means, that the hydrogen atoms are carrying a partial negative charge here. Although the point charge model is not suited to predict accurate g-values, this result is in line with the electronegativity differences, which are +0.35 (hydrogen positive) in the C-H bond and −0.35 (hydrogen negative) in the Si-H bond.

experimental $(1-\sigma_{av})g_I I$ values. The uncertainty in the resulting σ_{av}-values is thereby raised by ± 220 ppm.

When the σ_{av}-values determined here are compared with those calculated with the atomic-dipole approximation given by Gierke and Flygare [2], it is realized, that the agreement is very good for CH_3Br. This indicates, that Eq. (14) of [2] can successfully be used to calculate the nuclear shielding in bromine compounds. The agreement between observed and calculated σ_{av}-values is not so good for SiH_3Br. This might be explained by the special bonding situation in SiH_3Br ($p\pi$-$d\pi$-bonding), which is not accounted for in the calculated value. The difference in the σ_{av}-values is however only 1.2 standard deviations and so the atomic dipole approximation may still be applicable to SiH_3Br.

Paramagnetic Susceptibilities and Paramagnetic Shielding

The paramagnetic susceptibility $\chi_\parallel{}^p$ and the paramagnetic shielding $\sigma_\parallel{}^p$ are about three times as large for $SiH_3{}^{81}Br$ than they are for $CH_3{}^{81}Br$

Table 10. Molecular quantities derived from experimental data given in Table 6. The geometries of the nuclear frames are taken from Refs. [31] and [32]. The bulk magnetic susceptibilities are calculated from the Pascal constants [33], with an assumed uncertainty of $\pm 5\%$ for CH_3Br and — because of the special bonding situation — $\pm 10\%$ for SiH_3Br.

		$H_3Si^{81}Br$	$H_3C^{81}Br$
Molecular quadrupole moments in units of 10^{-26} esu cm^2			
$Q_{\parallel} = \frac{\lvert e\rvert}{2}\left\{\sum_n^{\text{nuclei}} Z_n(2z_n^2 - x_n^2 - y_n^2) - \langle 0\rvert\sum_\varepsilon^{\text{electrons}}(2z_\varepsilon^2 - x_\varepsilon^2 - y_\varepsilon^2)\lvert 0\rangle\right\}$	$Q_{\parallel}$	-0.1 ± 0.4	3.8 ± 0.9
$= -\frac{\hbar\lvert e\rvert}{4\pi M_p}\left\{\frac{g_{\parallel}}{A} - \frac{g_{\perp}}{B}\right\} - \frac{4mc^2}{\lvert e\rvert}\chi_{\parallel} - \chi_{\perp}$			
Second moments of the nuclear charge distribution calculated from the geometry of the nuclear frame. The units are Å^2.	$\sum_n Z_n z_n^2$	61.5 ± 0.1	30.84 ± 0.05
	$\sum_n Z_n x_n^2$	2.983 ± 0.004	1.687 ± 0.003
Paramagnetic susceptibilities in units of 10^{-6} erg/(G^2 mol)			
$\chi_{\parallel}^{p} = -\frac{N_L e^2}{2m^2c^2}\sum_\nu^{\text{ex. states}}\frac{\lvert\langle 0\rvert L_z\rvert\nu\rangle\rvert^2}{E_0 - E_\nu}$	$\chi_{\parallel}^{p}$	33.39 ± 0.05	10.11 ± 0.25
$= -\frac{N_L e^2}{4mc^2}\left\{\frac{\hbar}{4\pi M_p}\frac{g_{\parallel}}{A} - \sum_n^{\text{nuclei}} Z_n(x_n^2 + y_n^2)\right\}$	$\chi_{\perp}^{p}$	284.7 ± 0.5	139.3 ± 0.3
Diamagnetic susceptibilities in units of 10^{-6} erg/(G^2 mol)	$\chi_{\parallel}^{d}$	−87.6 ± 5.4	−61.4 ± 2.9
$\chi_{\parallel}^{d} = -\frac{N_L e^2}{4mc^2}\langle 0\rvert\sum_\varepsilon^{\text{electrons}}(x_\varepsilon^2 + y_\varepsilon^2)\lvert 0\rangle = \chi_{\parallel} - \chi_{\parallel}^{p}$.	$\chi_{\perp}^{d}$	−336.2 ± 5.8	−181.8 ± 2.9
Bulk susceptibility in units of 10^{-6} erg/(G^2 mol) $\chi = (\chi_{\parallel} + 2\chi_{\perp})/3$	χ	−52.4 ± 5.2	−45.4 ± 2.3
Second moments of the electronic charge distribution in Å^2			
$\langle 0\rvert\sum_\varepsilon^{\text{electrons}} z_\varepsilon^2\lvert 0\rangle = -\frac{2mc^2}{e^2}(2\chi_{\perp} - \chi_{\parallel})$	$\langle 0\rvert\Sigma z_\varepsilon^2\lvert 0\rangle$	68.9 ± 2.0	35.6 ± 1.0
$-\frac{\hbar}{8\pi M_p}\left(\frac{2g_{\perp}}{B} - \frac{g_{\parallel}}{A}\right) + \sum_n^{\text{nuclei}} Z_n z_n^2$	$\langle 0\rvert\Sigma x_\varepsilon^2\lvert 0\rangle$	10.3 ± 2.0	7.2 ± 1.0

(see Tables 6 and 10). Since the hydrogen atoms carry a partial negative charge in SiH_3Br, and because they are farther away from the symmetry axis in this molecule, the matrix elements $\langle 0\rvert L_z\rvert n\rangle$ will be larger for SiH_3Br. On the other hand, the energy differences between occupied and unoccupied states with π-symmetry appear to be slightly larger in SiH_3Br than in CH_3Br [22] and this should partly compensate the increase of the matrix-elements in the nominators of the perturbation sums. If we turn to the discussion of the $\chi_{\perp}^{p}$-values, we find that $\chi_{\perp}^{p}$ is only half as large in $CH_3{}^{81}Br$ as in $SiH_3{}^{81}Br$. To understand this we look at the definition of the paramagnetic susceptibility [9, 13]:

$$\chi_{\perp}^{p} \propto \sum_n^{\text{ex. states}} \frac{\lvert\langle n\rvert L_x\rvert 0\rangle\rvert^2}{E_n - E_0} = \frac{m}{2}\sum_\nu^{\text{nuclei}} Z_\nu(y_\nu^2 + z_\nu^2) - g_{\perp} I_{\perp}\frac{m}{2M_p}.$$

From the structure [31] and the $g_{\perp}$ and $I_{\perp}$ values (see Tables 3 and 6) one sees, that the second term on the right side contributes less than 10% to $\chi_{\perp}^{p}$. In other words, $\chi_{\perp}^{p}$ is mainly determined by the first "point charge" term, and because Z_ν is 14 for silicon and only 6 for carbon, and because the bond distances and hence the z_ν coordinates are slightly larger in SiH_3Br than in CH_3Br, this essentially explains the observed differences in the $\chi_{\perp}^{p}$-values. From the spin-rotation coupling constants $\sigma_{\perp}^{p}$ was found to be twice as large for $CH_3{}^{81}Br$ as for $SiH_3{}^{81}Br$ (see Table 6) and has been discussed already in [3].

Appendix I

Nonvanishing matrix elements of the nuclear quadrupole, $\mathcal{H}_Q$, spin-rotation, $\mathcal{H}_{SR}$, molecular Zeeman, $\mathcal{H}_g{}^{mol}$ and $\mathcal{H}_\chi$, nuclear Zeeman, $\mathcal{H}_g{}^{nucl}$, and translational Stark effect operators $\mathcal{H}_{TS}$ which were used in this work. The off diagonal matrix elements of $\mathcal{H}_{SR}$ and $\mathcal{H}_g{}^{nucl}$, not given in the literature, were derived by use of the Wigner-Eckart theorem.

$\mathscr{H}_{\mathrm{Q}}$

$$\langle J,K,I,M_J,M_I|\,\mathscr{H}_{\mathrm{Q}}\,|J,K,I,M_J,M_I\rangle = eQq\{3K^2/J(J+1)-1\}\cdot\{3M_J^2-J(J+1)\}\cdot\{3M_I^2-I(I+1)\}/\{4I(2I-1)(2J-1)(2J+3)\},$$

$$\langle J,K,I,M_J,M_I|\,\mathscr{H}_{\mathrm{Q}}\,|J,K,I,M_J\pm1,M_I\mp1\rangle = C_1\cdot(2M_J\pm1)(2M_I\mp1)\{(I\pm M_I)(I\mp M_I+1)(J\mp M_J)(J\pm M_J+1)\}^{1/2},$$

$$\langle J,K,I,M_J,M_I|\,\mathscr{H}_{\mathrm{Q}}\,|J,K,I,M_J\pm2,\ M_I\mp2\rangle = C_1\cdot\{(J\mp M_J)(J\pm M_J+1)(J\pm M_J+2)(J\mp M_J-1)(I\pm M_I)(I\mp M_I+1)\cdot(I\mp M_I+2)(I\pm M_I-1)\}^{1/2},$$

$$\langle J,K,I,M_J,M_I|\,\mathscr{H}_{\mathrm{Q}}\,|J+1,K,I,M_J,M_I\rangle = -C_2\cdot2M_J\{3M_I^2-I(I+1)\}\cdot\{(J+M_J+1)(J-M_J+1)\}^{1/2},$$

$$\langle J,K,I,M_J,M_I|\,\mathscr{H}_{\mathrm{Q}}\,|J+1,K,I,M_J\pm1,M_I\mp1\rangle = -C_2\cdot(2M_I\mp1)(J\mp2M_J)\cdot\{(I\pm M_I)(I\mp M_I+1)(J\pm M_J+1)(J\pm M_J+2)\}^{1/2},$$

$$\langle J,K,I,M_J,M_I|\,\mathscr{H}_{\mathrm{Q}}\,|J+1,K,I,M_J\pm2,M_I\mp2\rangle = \pm C_2\cdot\{(I\mp M_I+1)(I\mp M_I+2)(I\pm M_I-1)(I\pm M_I)(J\pm M_J+1)(J\pm M_J+2)\cdot(J\pm M_J+3)(J\mp M_J)\}^{1/2},$$

$$\langle J,K,I,M_J,M_I|\,\mathscr{H}_{\mathrm{Q}}\,|J+2,K,I,M_J,M_I\rangle = 2C_3\cdot\{3M_I^2-I(I+1)\}\cdot\{(J+M_J+1)(J+M_J+2)(J-M_J+1)\cdot(J-M_J+2)\}^{1/2},$$

$$\langle J,K,I,M_J,M_I|\,\mathscr{H}_{\mathrm{Q}}\,|J+2,K,I,M_J\pm1,M_I\mp1\rangle = 2C_3\cdot(1\mp2M_I)\cdot\{(I\pm M_I)(I\mp M_I+1)(J\mp M_J+1)(J\pm M_J+1)(J\pm M_J+2)\cdot(J\pm M_J+3)\}^{1/2},$$

$$\langle J,K,I,M_J,M_I|\,\mathscr{H}_{\mathrm{Q}}\,|J+2,K,I,M_J\pm2,M_I\mp2\rangle = C_3\cdot\{(I\pm M_I)(I\pm M_I-1)(I\mp M_I+1)(I\mp M_I+2)\cdot(J\pm M_J+1)(J\pm M_J+2)(J\pm M_J+3)(J\pm M_J+4)\}^{1/2}$$

with

$$C_1 = 3eQq\cdot\{3K^2/\{J(J+1)\}-1\}/\{8I(2I-1)(2J-1)(2J+3)\},$$

$$C_2 = 3eQq\cdot K[(J+K+1)(J-K+1)/\{(2J+1)(2J+3)\}]^{1/2}/\{8I(2I-1)J(J+1)(J+2)\},$$

$$C_3 = 3eQq\cdot[(J+K+1)(J+K+2)(J-K+1)(J-K+2)/\{(2J+1)(2J+5)\}]^{1/2}/\{16I(2I-1)(J+1)(J+2)(2J+3)\}.$$

$\mathscr{H}_{\mathrm{SR}}$

$$\langle J,K,I,M_J,M_I|\,\mathscr{H}_{\mathrm{SR}}\,|J,K,I,M_J,M_I\rangle = -C_{JK}M_JM_I,$$

$$\langle J,K,I,M_J,M_I|\,\mathscr{H}_{\mathrm{SR}}\,|J,K,I,M_J\pm1,M_I\mp1\rangle = -\tfrac{1}{2}C_{JK}\cdot\{[J(J+1)-M_J(M_J\pm1)][I(I+1)-M_I(M_I\mp1)]\}^{1/2}$$

with $C_{JK} = C_\perp - (C_\perp - C_\parallel)K^2/\{J(J+1)\}$.

$\mathscr{H}_{\mathrm{g}}^{\mathrm{mol}}$

$$\langle J,K,I,M_J,M_I|\,\mathscr{H}_{\mathrm{g}}^{\mathrm{mol}}\,|J,K,I,M_J,M_I\rangle = -\mu_N g_{JK}H_zM_J$$

with $g_{JK} = g_\perp - (g_\perp - g_\parallel)K^2/\{J(J+1)\}$, $\mu_N = e\hbar/2M_{\mathrm{p}}c$.

$\mathscr{H}_\chi$

$$\langle J, K, I, M_J, M_I | \mathscr{H}_\chi | J, K, I, M_J, M_I \rangle = -(\chi_\perp - \chi_\parallel) H_z^2 C_4 ,$$

$\mathscr{H}_g^{\text{nucl}}$

$$\langle J, K, I, M_J, M_I | \mathscr{H}_g^{\text{nucl}} | J, K, I, M_J, M_I \rangle = -\mu_N g_I (1 - \sigma_{\text{av}}) H_z M_I + \mu_N g_I (\sigma_\perp - \sigma_\parallel) H_z M_I \cdot 2 C_4 ,$$

$$\langle J, K, I, M_J, M_I | \mathscr{H}_g^{\text{nucl}} | J, K, I, M_J \pm 1, M_I \mp 1 \rangle = \mu_N g_I (\sigma_\perp - \sigma_\parallel) \cdot (2 M_J \pm 1) \cdot C_5 \cdot H_z \cdot \{[J(J+1) - M_J(M_J \pm 1)][I(I+1) - M_I(M_I \mp 1)]\}^{1/2}$$

with

$$C_4 = \{[3 M_J^2 - J(J+1)][J(J+1) - 3K^2]\} / \{3J(J+1)(2J+3)(2J-1)\} ,$$

$$C_5 = \{J(J+1) - 3K^2\} / \{2J(J+1)(2J-1)(2J+3)\} .$$

$\mathscr{H}_{\text{TS}}$

$$\langle J, K, I, M_J, M_I | \mathscr{H}_{\text{TS}} | J, K, I, M_J \pm 1, M_I \rangle = -\mu_{\text{el}} E_{\text{TS}} K \{J(J+1) - M_J(M_J \pm 1)\}^{1/2} / \{2J(J+1)\}$$

with

$E_{\text{TS}} = |(\boldsymbol{v}_0 \times \boldsymbol{H})/c|$,

$\boldsymbol{v}_0$ = translational velocity of the molecule with respect to the magnet,

c = velocity of light,

$\boldsymbol{H}$ = vector of the exterior magnetic field,

μ_{el} = ground state expectation value of the molecular electric dipole moment.

Appendix II. Nuclear Magnetic Moment of an Unshielded Br-Nucleus

The value of $g_I I_{(^{81}\text{Br})} = 2.2696(5)$ given in Ref. [21] is based on the measurements of Ref. [24] and [25], where the ratio of the NMR frequencies of the proton resonance and the $^{81}Br^-$-ion in an aqueous solution of KBr and NaBr at a given field was determined to be $0.27003 \pm 0.03\%$ and $0.27014 \pm 0.02\%$ respectively. In calculating the unshielded ^{81}Br nuclear magnetic moment from the measurements Mack [21] used a theoretical value of $\sigma^d = 3085$ ppm for the diamagnetic shielding and disregarded the paramagnetic shielding $\sigma^p_{(\text{aq. Br}^-)}$ for the Br^--ion in aqueous environment. From recent measurements of Lutz and coworkers [26] it becomes however possible to account for this paramagnetic contribution which can not be neglected. In the subsequent calculation of the $g_I I$-values for the bare nuclei we assume, that the values for the diamagnetic contributions to the bromine shielding in NaBr and KBr crystals, in dilute aqueous solutions, and in free atoms are sufficiently close to each other to neglect their differences [29]. We further assume, that the theoretical values for the paramagnetic contributions, σ^p, in NaBr and KBr [27] are sufficiently accurate to justify their use in the present calculation. Finally we assume that the theoretical value of the diamagnetic shielding in the free atom is also sufficiently accurate. With these assumptions, the derivation of the $g_I I$-values for the bare nuclei is straightforward as follows.

From Table 4 of Ref. [26] the differences in the experimental $\sigma_{\text{av}} = \sigma^p_{\text{av}} + \sigma^d_{\text{av}}$ values of the $^{79}Br^-$-ions in infinitely dilute aqueous solutions and in crystals are:

$$\sigma_{^{79}\text{Br}^-,\ \text{aq.}\ \infty,\ \text{av}} - \sigma_{^{79}\text{Br}^-,\ \text{NaBr, X-tal, av}} = -\ 6(5)\ \text{ppm} , \quad \text{(A.1)}$$

$$\sigma_{^{79}\text{Br}^-,\ \text{aq.}\ \infty,\ \text{av}} - \sigma_{^{79}\text{Br}^-,\ \text{KBr, X-tal, av}} = +\ 47(2)\ \text{ppm} . \quad \text{(A.2)}$$

With the assumption that the differences in the σ^d-values are negligible, these equations are equivalent to:

$$\sigma^p_{^{79}\text{Br}^-,\ \text{aq.}\ \infty,\ \text{av}} - \sigma^p_{^{79}\text{Br}^-,\ \text{NaBr, X-tal, av}} = -\ 6(5)\ \text{ppm} , \quad \text{(A.3)}$$

$$\sigma^p_{^{79}\text{Br}^-,\ \text{aq.}\ \infty,\ \text{av}} - \sigma^p_{^{79}\text{Br}^-,\ \text{KBr, X-tal, av}} = +\ 47(2)\ \text{ppm} . \quad \text{(A.4)}$$

Insertion of the theoretical values for $\sigma^p_{\text{X-tal}}$ from the work of Hafemeister and Flygare [27]

$$\sigma^{p}_{^{79}Br^-,\,NaBr,\,X\text{-}tal,\,av} = -470\ \text{ppm} \quad \text{and}$$
$$\sigma^{p}_{^{79}Br^-,\,KBr,\,X\text{-}tal,\,av} = -510\ \text{ppm}$$

yields:

$$\sigma^{p}_{^{79}Br^-,\,aq.\,\infty,\,av} = -476\ \text{ppm} \quad \text{[from Eq. (A.3)]}$$
$$\sigma^{p}_{^{79}Br^-,\,aq.\,\infty,\,av} = -463\ \text{ppm} \quad \text{[from Eq. (A.4)]}.$$

Of course both values should be identical. Their difference may give some hint as to the quality of the theoretical values and assumptions involved in their derivation. In the following we use $\sigma^{p}_{^{79}Br^-,\,aq.\,\infty,\,av} = -470 \pm 100$ ppm. The uncertainty of ± 100 ppm accounts for the fact, that theoretical values for $\sigma^{p}_{X\text{-}tal,\,av}$ have entered the value of $\sigma^{p}_{Br^-,\,aq.\,\infty,\,av}$ as well as the assumption of equal σ^{d}_{av}-values. In view of the fairly good agreement between the theoretical value for $\sigma^{p}_{X\text{-}tal,\,av}$ and the experimental value in the case of RbCl ($\sigma^{p}_{X\text{-}tal,\,exp,\,av} = -215(12)$ ppm [26] versus $\sigma^{p}_{X\text{-}tal,\,th.,\,av} = -190$ ppm [27]) we feel that our estimate of the uncertainty limit is rather conservative. If we now set $\sigma^{d}_{Br\text{-}atom,\,av} = 3121.2$ ppm [30] equal to $\sigma^{d}_{Br^-,\,aq.\,\infty,\,av}$ we arrive at:

$$\begin{aligned}\sigma_{Br^-,\,aq.\,\infty,\,av} &= \sigma^{p}_{Br^-,\,aq.\,\infty,\,av} + \sigma^{d}_{Br^-,\,aq.\,\infty,\,av}\\ &= -470 + 3121\ [\text{ppm}]\\ &= 2652\ \text{ppm}.\end{aligned}$$

Since this value is determined by the electronic surrounding of the bromine nucleus, it is, to a very good approximation, the same for both isotopes and may be used together with experimental values of Lutz and coworkers [28] to derive the final $g_I I$-values of the bare nuclei:

$$[(1 - \sigma_{Br^-,\,aq.\,\infty,\,av})\, g_I I_{(^{79}Br)}]_{exp} = 2.099047(4) \rightarrow g_I I_{(^{79}Br)} = 2.10463(21),$$

$$[(1 - \sigma_{Br^-,\,aq.\,\infty,\,av})\, g_I I_{(^{81}Br)}]_{exp} = 2.262636(4) \rightarrow g_I I_{(^{81}Br)} = 2.26865(23).$$

The uncertainties are essentially due to the 100 ppm uncertainty assumed for $\sigma_{Br^-,\,aq.\,\infty,\,av}$.

With these improved values we can recalculate the observed nuclear shielding constants for methyl- and silylbromide:

	$[(1 - \sigma_{av})\, g_I I]_{exp}$	σ_{av}/ppm	σ^{calc}_{av}/ppm
$H_3C^{81}Br$	2.2640(3)	2050(440)	2502
$H_3Si^{81}Br$	2.2615(4)	3150(480)	2817

Now the observed and calculated shielding constants of H_3CBr *and* H_3SiBr agree within one standard deviation.

Wir danken Herrn Prof. Dr. H. Dreizler für die kritische Durchsicht des Manuskripts. Der Deutschen Forschungsgemeinschaft sei für die Bereitstellung von Sach- und Personalmitteln gedankt. Die numerischen Rechnungen wurden auf der PDP-10-Anlage des Rechenzentrums der Christian-Albrechts-Universität durchgeführt.

[1] D. L. Vanderhart and W. H. Flygare, Mol. Phys. **18**, 77 (1970).
[2] T. D. Gierke and W. H. Flygare, J. Am. Chem. Soc. **94**, 7277 (1972).
[3] K.-F. Dössel and D. H. Sutter, Z. Naturforsch. **32a**, 1444 (1977).
[4] D. Sutter, Z. Naturforsch. **26a**, 1644 (1971).
[5] S. G. Kukolich, J. Chem. Phys. **55**, 4488 (1971).
[6] Z. F. Slawsky and D. M. Dennison, J. Chem. Phys. **7**, 509 (1939).
[7] W. Gordy and R. L. Cook, Microwave Molecular Spectra, Interscience Publishers, John Wiley, New York 1970, Sect. 9.4.
[8] W. Hüttner and W. H. Flygare, J. Chem. Phys. **44**, 4137 (1967).
[9] W. H. Flygare, Chem. Rev. **74**, 653 (1974).
[10] L. Engelbrecht and D. H. Sutter, Z. Naturforsch. **30a**, 1265 (1975).
[11] Ref. [7], Appendix III.
[12] M. Suzuki and A. Guarnieri, Z. Naturforsch. **31a**, 1242 (1976).
[13] D. H. Sutter and W. H. Flygare, Topics in Current Chemistry **63**, 89 (1976), Sect. III, E.
[14] loc. cit., Sect. III, B.
[15] J. Demaison, A. Dubrulle, D. Boucher, and J. Burie, J. Chem. Phys. **67**, 254 (1977).
[16] Ref. [7], p. 658.
[17] Ref. [7], p. 398.
[18] I. Ozier, S. S. Cel, and N. F. Ramsey, J. Chem. Phys. **65**, 3985 (1976).
[19] R. L. Shoemaker and W. H. Flygare, J. Am. Chem. Soc. **94**, 684 (1972).
[20] Ref. [7], p. 671.
[21] J. E. Mack, Rev. Mod. Phys. **22**, 64 (1952).
[22] G. C. Causley, J. B. Clark, and B. R. Russel, Chem. Phys. Lett. **38**, 602 (1976).
[23] K. Kawaguchi, C. Yamada, T. Tanaka, and E. Hirota, J. Mol. Spectry. **64**, 125 (1977).
[24] F. Bitter, Phys. Rev. **75**, 1326 (1949).
[25] J. R. Zimmerman and D. Williams, Phys. Rev. **76**, 350 (1949).
[26] W. Gauss, S. Günther, A. R. Haase, M. Kerber, D. Kessler, J. Kronenbitter, H. Krüger, O. Lutz, A. Nolle, P. Schrade, M. Schüle, and G. E. Siegloch, Z. Naturforsch. **33a**, 934 (1978).
[27] D. W. Hafemeister and W. H. Flygare, J. Chem. Phys. **44**, 3584 (1966).

[28] J. Blaser, O. Lutz, and W. Steinkilberg, Z. Naturforsch. **27a**, 72 (1972).
[29] A. Saika and C. P. Slichter, J. Chem. Phys. **22**, 26 (1954).
[30] G. Malli and C. Froese, Int. J. Quant. Chem. **15**, 95 (1967).
[31] R. Kewley, P. M. McKinney, and A. G. Robiette, J. Mol. Spectry. **34**, 300 (1970).
[32] S. L. Miller, L. C. Aamodt, G. Dousmanis, C. H. Townes, and J. Kraitchman, J. Chem. Phys. **20**, 1112 (1952).
[33] H. F. Hameka, Advanced Quantum Chemistry, Addison-Wesley Publ. Co., Reading (Mass.) 1965, p. 180.